

Application Research of Sonar Detection Method in Melting Exploration at the Bottom of Piles

Tianzhi Liu¹, Ke Tu^{2*}, Chunsong Duan¹, Qian Chen¹, Liu Hu Yan¹

¹Yunnan Infrastructure Investment Co.,Ltd., Kunming 650217, Yunnan Province, China

²China Merchants Chongqing Highway Engineering Testing Center Co., Ltd., Chongqing 400060, China

*Corresponding author: Ke Tu, 406244561@qq.com

Copyright: © 2023 Author(s). This is an open-access article distributed under the terms of the Creative Commons Attribution License (CC BY 4.0), permitting distribution and reproduction in any medium, provided the original work is cited.

Abstract: Karst landforms are widely distributed in China, and are most common in Yunnan, Guizhou and Guangxi. If the development of karst caves at the bottom of the piles cannot be accurately ascertained before the construction of bridge pile foundations, accidents such as hole collapse, slurry leakage, and drill sticking will easily occur. In this paper, the principle and method of sonar detection for detecting karst caves at the bottom of bridge piles was introduced, and the sonar detection data and the cave situation at the bottom of the pile during the construction process in combination with the case of Yunnan Zhengguo Highway Project was analyzed, which verifies the practicability and reliability of sonar detection method reliability.

Keywords: Principle of sonar detection method; General situation of sonar detection method engineering

Online publication: July 28, 2023

1. Introduction

Karst, also known as karst landform, refers to the special landform and hydrogeology formed by soluble rock formations (mostly carbonate rocks, sulfate rocks, etc.) under the action of geological forces (especially the erosion of surface water and groundwater). Karst landforms are widely distributed around the world, and China is one of the countries with the most karst landforms. In China, places like Yunnan, Guizhou and Guangxi have the most karst landforms^[1]. Karst areas often have irregular distribution and filling of karst caves, which will cause highly varied developments of the caves. The soil properties of the shallow soil surface do not meet the load-bearing and deformation requirements of shallow foundations, thus punching grouting or manual excavation piles are often used. Construction in karst areas without fully ascertaining the karst caves are very high risk, and serious accidents such as hole collapse, slurry leakage, ground subsidence, and drill sticking are prone to occur^[2].

Therefore, before the construction of the pile foundation, detailed and accurate exploration of the karst cave at the bottom of the piles is required to avoid the above accidents during construction. Commonly used cave detection methods include high-density apparent resistivity method, shallow seismic method, bottom-penetrating radar method, advanced drilling method, elastic wave CT method, tube wave testing method, sonar detection method, etc.^[3]. Among them, the resistivity method utilizes the different conductive properties of underground layers, and detects the distribution of geological layers according to the different conduction laws of current under the action of an external electric field^[4]. The shallow seismic method utilizes the different characteristics of wave impedance between different geological layers, and detects information such as the position, size, and orientation of caves according to the different reflection waveforms of stress waves at different layers^[5]. However, these two methods are difficult to use in mud,

and are not suitable for bored piles. If used for detection before drilling, they cannot accurately detect the position of the cave. The CT method uses elastic waves to project the geology, and calculates the position of the cave through the attenuation of elastic waves in different geological layers. However, this method requires at least two boreholes around the pile and is easily disturbed during detection^[6]. As compared to the diameter of the pile, the diameter of the drilled hole by the advanced drilling method is too small, making it easy to miss the karst cave, moreover multiple drillings are time-consuming and laborious^[7].

The commonly used methods are ground penetrating radar and sonar. The ground penetrating radar method uses the ground radar to emit high-frequency electromagnetic waves, and judges the condition of the cave through the amplitude, phase, and waveform of the reflected waveforms between different geological layers. However, the ground penetrating radar method is mostly used for piles before drilling or manual excavation, and is not suitable for mud^[8]. The sonar detection method can utilize mud as a coupling agent, making it an interference medium to propagate sound waves. This allows the waves to go deep into the pile diameter hole during the construction stage and directly conduct close-range and high-precision detection at the bottom of the piles. This method can be applied to both manual excavation piles and bored piles^[9].

Based on the newly-built highway in Zhenxiong, Zhaotong, Yunnan, the sonar detection method is used for the new pile foundation. Through the comparison of the collected data of sonar detection method and ground penetrating radar method, the applicability and accuracy of the sonar detection method were verified.

2. Principle of sonar detection method

2.1. Sonar detection method

Sonar detection method works by emitting sonar stress waves. According to different impedances between different soil layers, sonar waves have different amplitudes and strengths when passing through different layers, which provides data about the direction of pile bottom culverts and other information. During on-site detection, the electrical signal emitted by the host is first converted into an acoustic signal by the sonar transducer and emitted vertically downward. The acoustic signal then travels down through the mud and bedrock. Because the resistivity of caves or weak interlayers under the bedrock is different from that of the bedrock, sonar signals generate strong reflection waves. Finally, the reflected waves are received by the three receiving probes around the transmitting probe, as shown in **Figure 1**. The pitch and roll angles of the three receiving probes are measured by the three-dimensional electronic compass in the probe to ensure that the sound wave signal is transmitted to the surrounding rock at the bottom of the piles as vertically as possible. The receiving transducer converts the acoustic signal into an electrical signal and transmits it to the on-site host for display, analysis and storage^[9]. The detection process is shown in **Figure 2**.

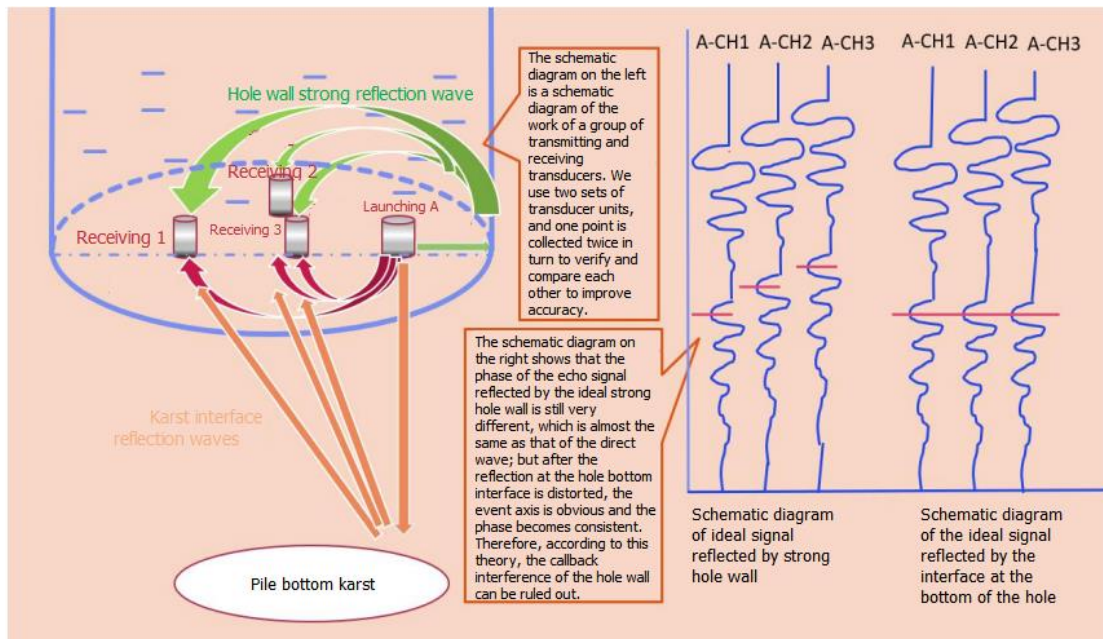


Figure 1. Schematic diagram of sonar detection method

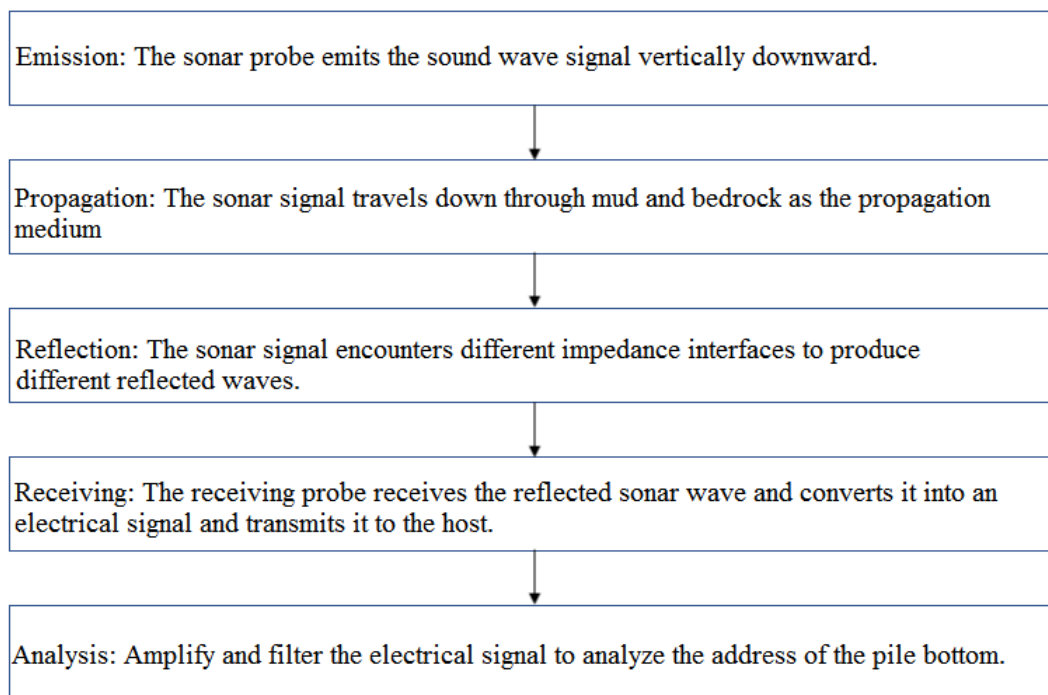


Figure 2. The detection process of the sonar detection method

2.2. Sonar detection theory

Because the distance between the transmitting probe and the receiving probe of the sonar detector is relatively close, it can be regarded as a very small offset. Therefore, one-dimensional wave theory^[10] can be used for analysis. Its theoretical vibration equation is as follows:

$$\frac{\partial^2 u}{\partial t^2} = C^2 \frac{\partial^2 u}{\partial x^2} \quad (1)$$

where u represents the particle vibration position, t represents the time, x represents the particle vibration direction, and C represents the wave propagation velocity of the particle in the x direction. From calculations of Equation (1), a D'Alembert's solution like Equation (2) can be obtained to show that the vibration of the particle is the superposition of two reverse waves:

$$u(x, t) = f(x - Ct) + g(x + Ct) \quad (2)$$

assuming that $f(x - Ct)$ is the downward-firing sonar stress wave and $g(x + Ct)$ is the reflected wave from different interfaces. They maintain the original waveform, propagate and superimpose with speed C . When the sonar stress wave encounters soil interface with different properties above and below, the stress wave will be refracted and reflected. Its reflection must have equal stress on both sides of the interface and continuous particle velocity. This can be reflected as Equation (3) and (4):

$$P + P_R = P_T \quad (3)$$

$$v - v_R = v_T \quad (4)$$

where P , P_R , P_T represents the incident, reflected, and transmitted sound pressures respectively, and v , v_R , v_T represents the incident, reflected, and transmitted wave velocities respectively. Equation (5) can be obtained by substituting $v = P/Z$ into Equation (4), where Z is the wave impedance of the medium and can be represented as $Z = \rho C$:

$$\frac{P}{Z_{top}} - \frac{P_R}{Z_{bottom}} = \frac{P_T}{Z_{bottom}} \quad (5)$$

By solving Equation (3) and (5) simultaneously, Equation (6) is obtained:

$$R = \frac{P_R}{P} = \frac{Z_{bottom} - Z_{top}}{Z_{bottom} + Z_{top}} \quad (6)$$

where R is the reflection coefficient, which represents the difference in wave impedance between soil layers, indicating the situation at the bottom of the pile. The greater the absolute value of R , the greater the difference in wave impedance between the upper and lower media. As shown in **Table 1**.

Table 1. Reflection coefficient reflects bedrock conditions

$R > 0$	$R < 0$	$R = 0$ and the signal energy is strong	$R = 0$ and the signal energy is weak
Bedrock is soft at the top and hard at the bottom	Cave development	Bedrock intact	Bedrock shattering

When the bedrock at the bottom of the pile is complete, the sonar stress wave does not undergo secondary reflection, that is, $R = 0$, and the signal energy is strong. Ideally, the time-domain curve of the reflected wave received by the sonar receiving probe decays exponentially, and the amplitude decays uniformly. When there is a karst cave at the bottom of the pile, because the wave impedance of the filling in the karst cave is smaller than that of the bedrock at the top of the karst cave, that is, $R < 0$, the phase of the reflected wave is opposite to that of the incident at the bottom of the pile, and a quadratic wave impedance will appear on the time domain curve. Reflection, superimpose the reverse bit waveform at the cave development. When there is a harder rock layer at the bottom of the pile that is soft at the top and hard at the bottom, the density of the rock medium in the lower layer is higher, and its wave impedance is greater than that of the upper bedrock. At this time, $R > 0$, and the phase of the reflected wave at the interface is the same as that of the incident at the bottom of the pile. The reflected waves are the same, shown on the time domain curve as positive phase waveform superposition. When the rock formation at the bottom of the pile is broken, the bedrock at the bottom of the pile does not have a clear and complete reflection surface, at this time $R = 0$ but the signal energy is weak. The signal received by the sonar receiver is much weaker than when the bedrock is intact ^[10].

2.3. Sonar detection device

The sonar detector used in this paper is JL-SONAR(B), which includes a field host for controlling the probe and analyzing data, a cable connecting the host and the probe, and a sonar probe. Wherein the sonar probe includes a microcomputer, a transmitting probe, a receiving probe and a three-dimensional electronic compass. The micro-computing realizes the transmission and control of each instruction. The three-dimensional electronic compass is installed horizontally in the sonar probe to measure the azimuth and inclination angle of the probe. The transmitting power of the transmitting probe can reach 10 kW, and the transmitting frequency band is 200 Hz to 8 kHz. The detection accuracy is ensured by high-frequency emission, and the high-frequency part is not rapidly attenuated by high power. The detector is shown in **Figure 3**.



Figure 3. Sonar detector

3. Engineering example of sonar detection method

3.1. Project overview

Zhenxiong County is located in the hinterland of Wumeng Mountain, where roads are the main means of transportation. The Zhenxiong-Guozhu Railway Station-Dawan Highway Project is located in Zhenxiong County, Zhaotong City, Yunnan Province. The terrain where the railway line passes has large ups and downs, varies greatly and is very complex. It is dominated by karst landforms, which can be classified according to their origin and morphology into denuded low-middle level landforms, erosive accumulation landforms, and tectonic dissolution low-middle mountain landforms. On the other hand, the fractures in the rock joints of the middle mountain landform with low tectonic dissolution are extremely developed, and

the rock mass is severely broken. Therefore, the flow of groundwater is complicated, which provides good conditions for the development of karst caves. Moreover, the expressway crosses many rivers and valleys, so the scale of the bridge is relatively large. The piers and abutments under the bridge are mainly based on pile foundations, and most of the pile foundations are stressed by the pile tip resistance. Therefore, there is a strong demand for detection of the development of karst caves at the pile bottom. It is necessary to detect whether there is a karst cave within three times the pile diameter below the under pile and not less than 5 m.

3.2. Complete typical data of pile foundation surrounding rock

The detection results of a pile foundation on Zhenxiong Highway are shown in **Figure 4**. The pile foundation was an end-bearing pile, and the impact hole was used. The designed pile length was 27.0 m and the pile diameter was 1.8 m. From the detection data in **Figure 4**, it can be seen that the reflected waveform of the pile foundation was regular, and the overall attenuation was normal. It can be seen that $R = 0$, and the signal energy was strong. Based on this, it was inferred that the surrounding rock at the bottom of the pile foundation was complete, and the bearing capacity of the surrounding rock was relatively high. No karst caves have been found within the range below the pile bottom elevation of 6m. It was recommended to proceed to the next step.

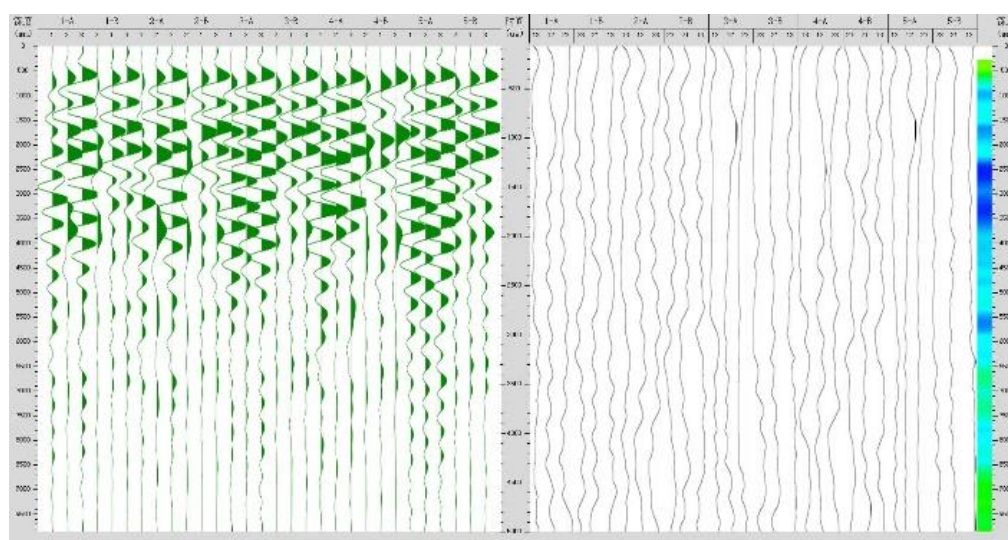


Figure 4. Detection results of an impact-drilled end-bearing pile foundation on Zhenguo Highway

3.3. Typical data of fissure development in pile bottom surrounding rock

The detection results of a pile foundation on Zhenguo Highway are shown in **Figure 5**. The pile foundation was a rock-socketed pile, which was drilled by impact. The designed pile length was 20.0 m and the pile diameter was 1.6 m. From the detection data in **Figure 5**, it can be seen that the waveform of the pile foundation was regular, the attenuation was relatively normal, and a weak positive phase high-frequency reflection signal appeared within the range of 1.5 m to 2.5 m of the pile bottom elevation. It can be seen that at this time $R > 0$, the bedrock at the pile bottom was soft at the top and hard at the bottom. Based on this, it was speculated that the surrounding rock at the bottom of the pile foundation has local cracks and weak interlayers, and no karst caves have been found within 5.0 m below the pile bottom elevation. Moreover, the positive phase reflection of the pile foundation waveform was weak, and the weak interlayer had little influence on the bearing capacity of the surrounding rock at the bottom of the pile. It was recommended to proceed to the next step.

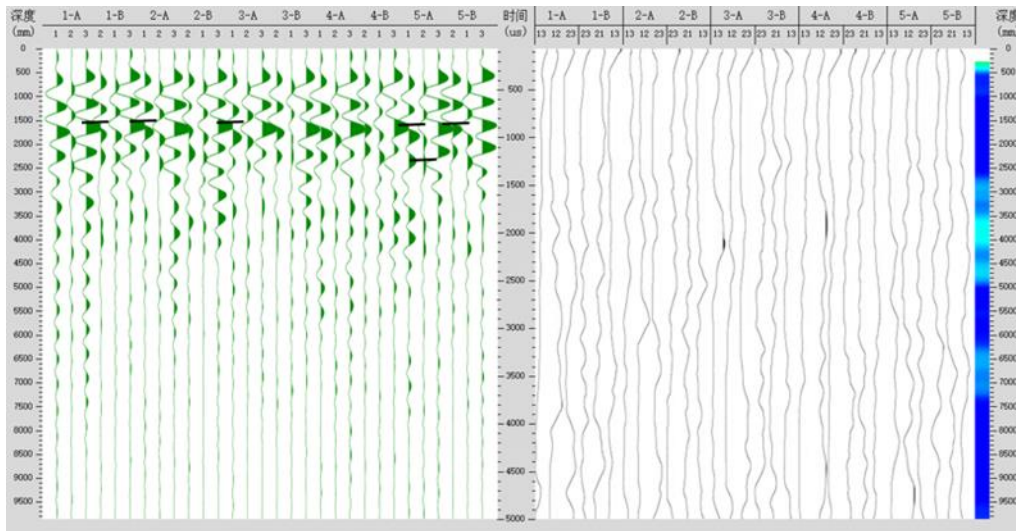


Figure 5. Detection results of an impact-drilled rock-socketed pile foundation on Zhengguo Highway

3.4. Typical data of pile bottom surrounding rock crushing

The detection results of a pile foundation on Zhengguo Highway are shown in **Figure 6**. The pile foundation was a rock-socketed pile, which was manually dug. The designed pile length was 20.0 m and the pile diameter was 1.6 m. From the detection data in **Figure 6**, it can be seen that the waveform of the pile foundation was irregular and the attenuation was abnormal. There were obvious random reflection signals in the range of 2.0 m to 3.0 m at the bottom of the pile, and the waveform energy was weakened below 5.0 m. It can be seen that $R > 0$, and the energy signal weakened significantly. Based on this, it was speculated that the surrounding rock at the pile bottom in the range of 2.0 m to 3.0 m below the pile bottom elevation of the pile foundation is relatively broken, but it has little impact on the load capacity of the pile bottom surrounding rock. No karst caves were found within 5.0 m below the pile bottom elevation. It was recommended to proceed to the next step.

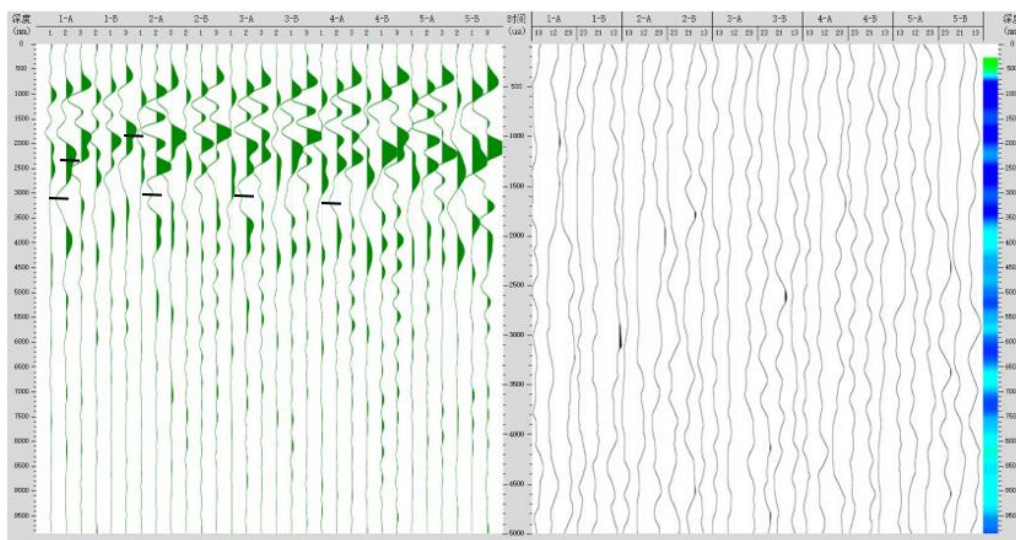


Figure 6. Detection results of a manually dug rock-socketed pile foundation on Zhengguo Highway

3.5. Typical data on the development of karst caves in surrounding rocks at the bottom of piles

The detection results of a pile foundation on Zhengguo Highway are shown in **Figure 7**. The pile foundation was end-loaded, and impact holes were used. The designed pile length was 18.0 m and the pile diameter was 2.2 m. From the detection data in **Figure 7**, it can be seen that the frequency of the pile foundation

detection waveform data was low, the waveform was irregular, and the attenuation was abnormal. In the southwest direction of the pile bottom, there were strong low-frequency reflection signals and strong negative phase reflection signal, which show that $R < 0$ at this time. Based on this, it was speculated that karst caves have occurred within the range of 1.5 m to 2.5 m below the southwest elevation of the pile foundation. It was suggested that the pile foundation should be deepened by 2.5 m to pass through the cave. During the deepening process, due to the existence of caves, there was a slurry leakage situation. This also proves the accuracy of the sonar detection method.

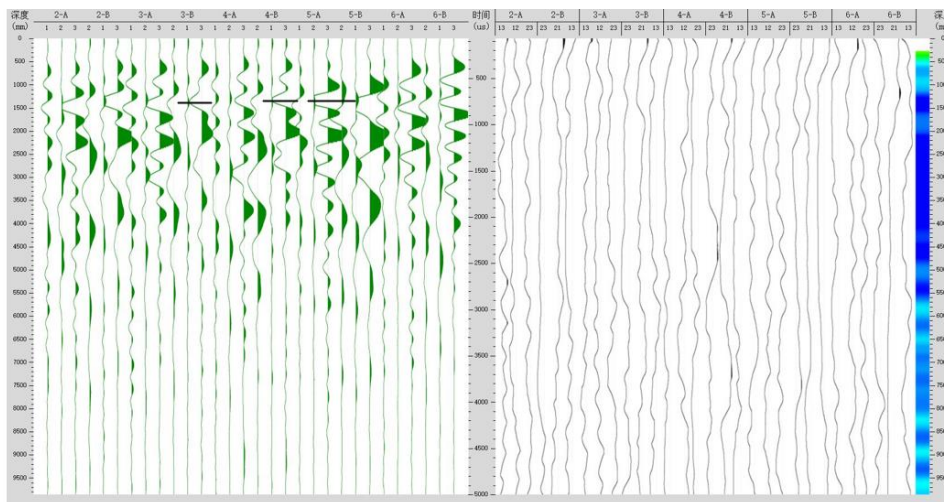


Figure 7. Detection results of an impact-drilled end-loaded pile foundation on Zhengguo Highway

After the pile foundation was deepened by 2.5 m, retesting was carried out, and the results are shown in **Figure 8**. At the time, the actual excavation depth was 22.30 m. From the detection graph, it can be seen that the abnormal points were significantly reduced after the pile foundation was deepened, the waveform was relatively regular, and the attenuation was basically normal. It can be seen that $R = 0$ at this time, and the signal energy was strong. In the range of 2.0 m to 3.0 m below the southern elevation of the pile bottom, the waveform signal was weak, and it can be seen that $R = 0$ at this time, and the signal energy was weak. Based on this, it is inferred that local cracks were developed in the rock strata within 2.0 m to 3.0 m below the southern elevation of the pile foundation, and the pile base rock is relatively complete in other positions. No karst caves have been found 8 m below the pile bottom.

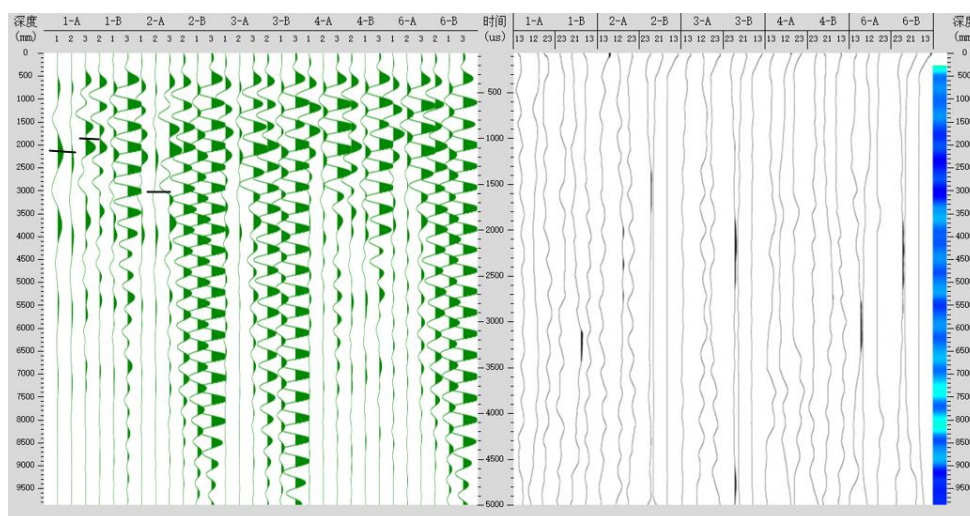


Figure 8. The detection results of a pile foundation deepened by 2.5 m on Zhengguo Highway

The detection results of another pile foundation on the Zhengguo Highway are shown in **Figure 9**. The pile was a rock-socketed pile, which was manually dug. The designed pile length was 20.0 m and the pile diameter was 1.6 m. From the detection data in **Figure 9**, it can be seen that the waveform of the pile bottom of the pile foundation was irregular, the attenuation was abnormal, and a strong low-frequency negative phase reflection signal appeared within the range of 1.5 m to 3.0 m of the pile bottom elevation. It can be seen that $R < 0$ at this time, the surrounding rock at the bottom of the pile was hard at the top and soft at the bottom, and the signal energy was weak. Based on this, it was speculated that the suspected karst caves developed within the elevation range of 1.5 m to 3.0 m southwest of the pile bottom of the pile foundation, and the surrounding rock at the pile bottom was severely broken within the range of 1.5 m to 3.0 m at the pile bottom. It was recommended to deepen the tunnel by 3.0 m.

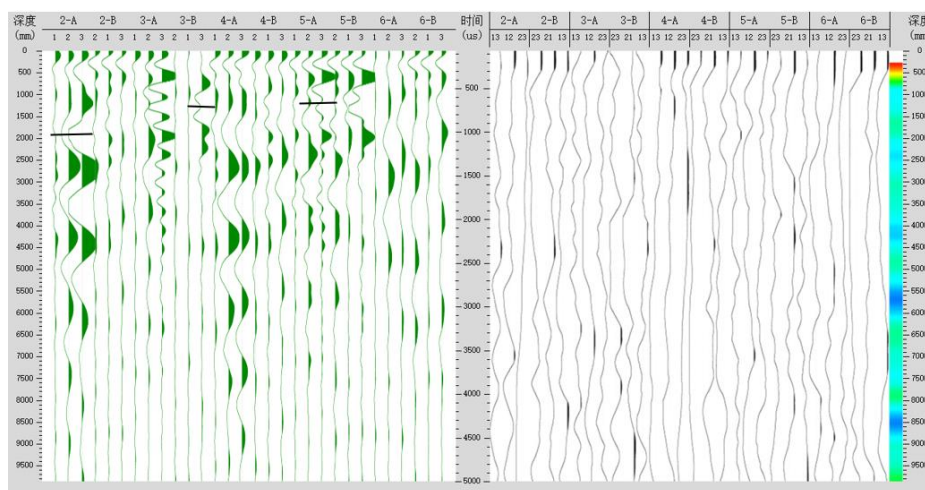


Figure 9. Detection results of another pile foundation on Zhengguo Highway

The slag sample at the bottom of the pile manually excavated is shown in **Figure 10**. The order of the slag samples is that the slag sample box is sorted from left to right, from top to bottom, and each grid represents 1 meter of slag samples. It can be seen from the slag sample diagram that the pile bottom of the pile foundation was mainly composed of silty clay, and the soil quality of the pile bottom is shown in **Figure 11**. It can be seen that the bottom of the pile was still dominated by silty clay mixed with gravel, and the surrounding rock at the bottom of the pile was severely broken, which also verifies the accuracy of the sonar detection method.



Figure 10. Slag sample at pile bottom



Figure 11. Soil sample at pile bottom

The detection results after the pile foundation was deepened by 3.0 m is shown in **Figure 12**. From the detection data in the figure, it can be seen that the abnormal points of the pile foundation were reduced, but the signal energy was weak, and the waveform attenuation can be found. It can be seen that at this time

$R = 0$, the signal energy was weak, and it is speculated that the surrounding rock at the bottom of the pile was broken. However, there were no caves, and the fracture was not serious and can still be used as a bearing layer.

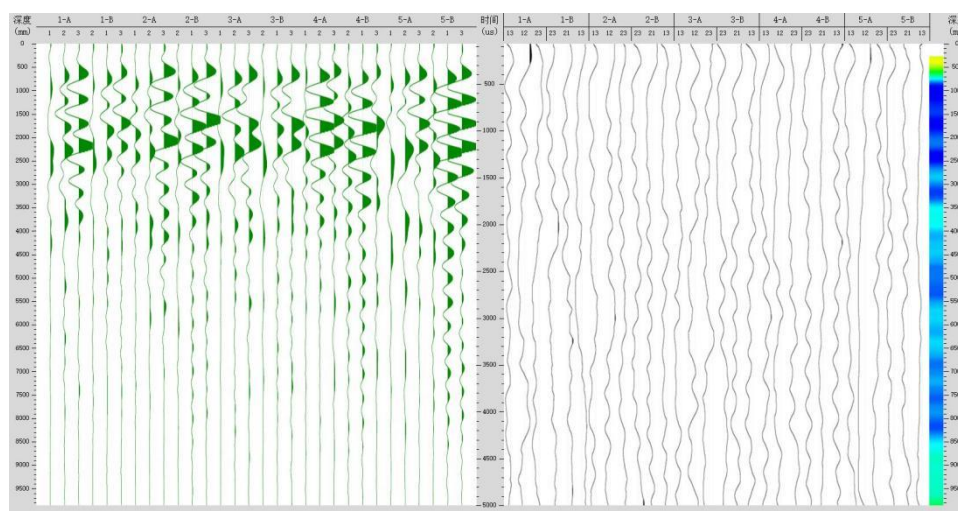


Figure 12. The detection results of a pile foundation deepened by 3 m on Zhengguo Highway

4. Conclusion

4.1. Advantages of sonar detection

The sonar detection method does not require advanced geological drilling, and the operation method is simple. It does not need to drill holes in advance, and can complete pile-by-pile detection. The detection cost is low, and the detection results are accurate and reliable. It overcomes the shortcomings of other detection methods, such as complicated operation, high cost, and inaccurate detection.

In addition, mud in bored piles may hinder other detection methods and affect the accuracy of detection results. The sonar detection method uses mud as the coupling medium, and the acoustic impedance of the mud is closer to the rock, which can improve the acoustic coupling rate, so that more acoustic energy can be transmitted into the bedrock at the pile bottom.

4.2. Disadvantages of sonar detection

Although the sonar detection method can detect the condition of the surrounding rock at the bottom of the pile and determine whether there are karst caves developed, the signal gradually weakens due to the increase of the sound wave signal with the depth of the surrounding rock. When the depth of the cave is deep, the height of the cave cannot be accurately detected, and the specific development conditions such as the width and filling status of the cave cannot be accurately measured through a single point. There is also a need to continue to improve detection techniques.

In the artificial excavated pile, because of the lack of mud as the coupling medium, the sonar energy in the artificial excavated pile cannot be well transmitted to the bottom of the pile, resulting in weak acoustic reflection signals received.

Disclosure statement

The authors declare no conflict of interest.

References

- [1] Yang Y, Liu H, Huang X, et al., 2022, Analysis of DC Resistivity Anomaly Characteristics and Research on Terrain Correction Method under Complex Terrain Conditions. *Hongshuihe*, 41(06): 118–123.
- [2] Wu Q, Yao X, Chen X, et al., 2022, Research on Non-destructive Detection Method of Soil Configuration based on Ground Penetrating Radar. *Arid Region Geography*, 45(06): 1860–1869.
- [3] Gao J, Zhou T, Du W, et al., 2022, Research on Multi-echo Detection Method of Multi-beam Bathymetric Sonar based on Phase Feature. *Journal of Instrumentation*, 43(08): 193–203. <http://doi.org/10.19650/j.cnki.cjsi.J2209721>
- [4] Song Y, 2022, Application of Shallow Seismic Reflection Wave Method in Site Selection and Investigation of Road Engineering. *Metallurgical Management*, 2022(07): 115–117.
- [5] Peng Z, Song W, 2021, Research on Construction Technology of Pile Bottom Exploration and Dissolution in Karst Landform. *Traffic World*, 2021(23): 163–164. <http://doi.org/10.16248/j.cnki.11-3723/u.2021.23.068>
- [6] Fang Y, Wu Z, Sheng Q, et al., 2020, Intelligent Identification Method of Tunnel Stratum Based on Advanced Drilling Test. *Rock and Soil Mechanics*, 41(07): 2494–2503.
- [7] Zhou K, Wang H, 2018, Application of Cross-hole CT Method in Pile Foundation Spacing Detection in Subway Engineering. *Tunnel Construction (Chinese and English)*, 38(05): 747–752.
- [8] Liu C, Shi Z, Liu L, et al., 2017, A Review of Pile Karst Detection Methods in Complex Karst Areas. *Proceedings of the 15th National Academic Conference on Engineering Geophysical Prospecting and Geotechnical Engineering Testing*, 11–17.
- [9] Shi Z, Liu L, Peng M, et al., 2016, Sonar Detection Method and Application Research on Karst Caves at the Bottom of Bored Piles. *Journal of Rock Mechanics and Engineering*, 35(01): 177–186. <http://doi.org/10.13722/j.cnki.jrme.2015.0125>
- [10] Shi X, 2005, Study on the Roof Stability of Hidden Karst Cave Under Pile Foundation Load in Karst Area, dissertation, Graduate School of Chinese Academy of Sciences (Wuhan Institute of Rock and Soil Mechanics).

Publisher's note

Bio-Byword Scientific Publishing remains neutral with regard to jurisdictional claims in published maps and institutional affiliations.